

Supporting Information

Diffusion Limited Cryopreservation of Tissue with Radiofrequency Heated Metal Forms

Zonghu Han, Anirudh Sharma[†], Zhe Gao[†], Timothy W. Carlson, M. Gerard O'Sullivan, Erik B. Finger, John C. Bischof^{*‡}

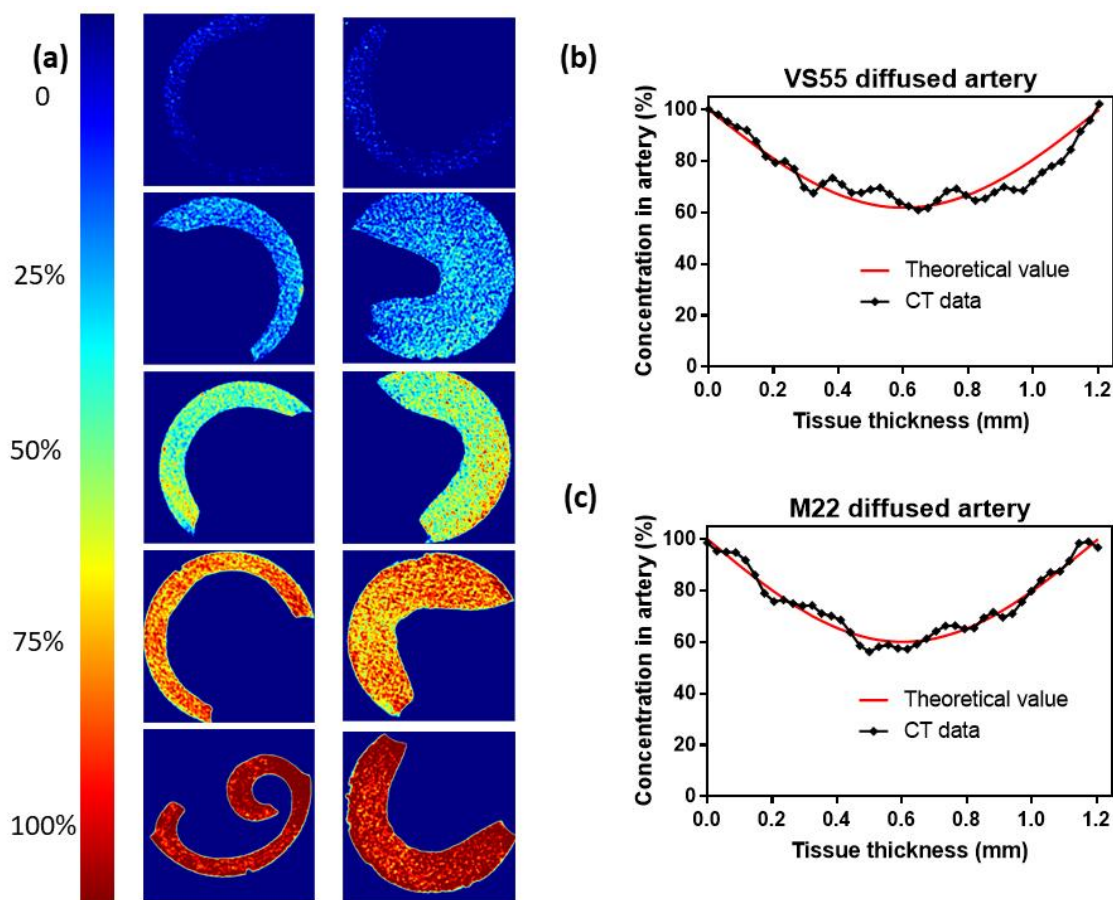


Figure S1. (a) Pseudocolor image for arteries equilibrated by diluted CPA (0 – 100%, 0 means solely carrier solution and 100% represents full strength CPA). The series of figure on the left side is for VS55 diffused carotid artery, on the right side is for M22 diffused aorta. (b, c) Two examples of CPA distribution after 15 min step loading on cross section obtained by μ CT compared to theoretical values obtained by best fit diffusivity. (b) Best fit diffusivity for this VS55 diffused sample is $7.0 \times 10^{-11} \text{ m}^2/\text{s}$, $R^2=0.86$. (c) Best fit diffusivity for this M22 diffused sample is $6.7 \times 10^{-11} \text{ m}^2/\text{s}$, $R^2=0.96$.

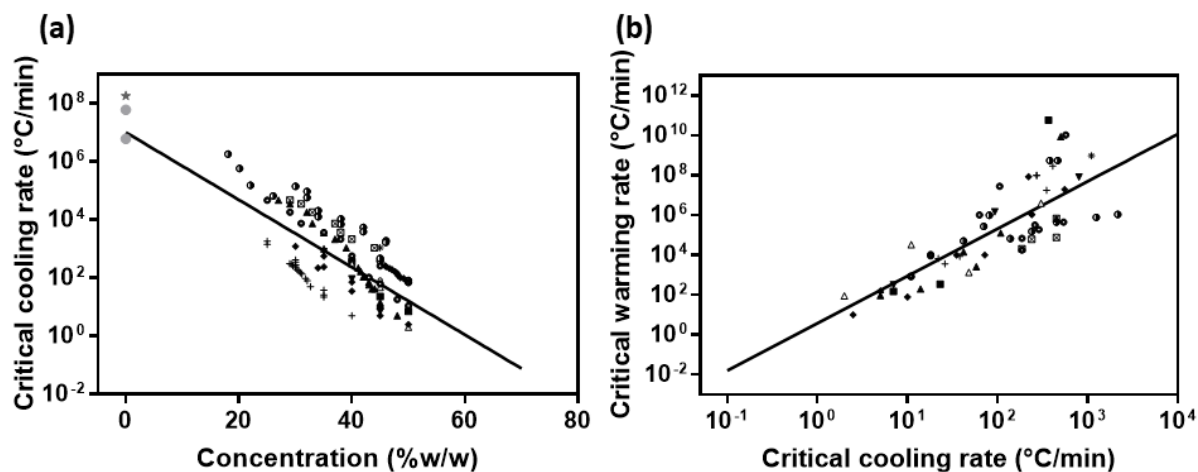


Figure S2. Re-plot of the figure in reference [26], Z. Han, J. Bischof, *CryoLetters* 2020, 41, 185. (a) CCRs for solutions of CPAs in water in relation to their concentrations. (b) CWRs as a function of CCRs for solutions of CPAs in water. Symbols: ★: Water estimated by Bald, ●: Water estimated by Bruggeller and Mayer, +: 2,3-Butanediol, ◆: 1,2-Propanediol, ○: Ethylene glycol, ▲: Dimethyl sulfoxide (DMSO), ◐: Glycerol, ▼: 1,3-Butanediol, △: 1,2,3-Butanetriol, △: Diethylformamide (DEF), ■: dimethylformamide (DMF), ♀: 1,4-Butanediol, *: 1,3-Propanediol, ☒: PEG 200

The supplemental histology data are shown in Figure S3-8. Figure S3 and S4 show control aortas, and Figure S5 to S8 show vitrified aortas. The findings are consistent with the descriptions in the main text.

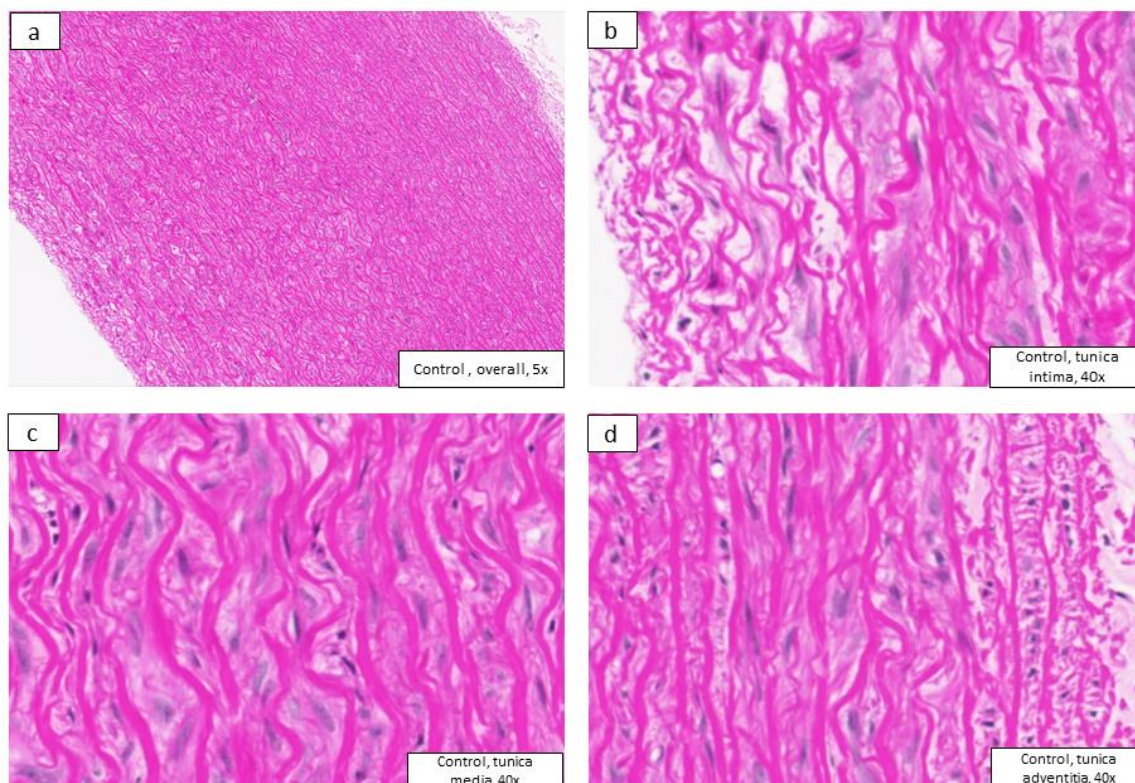


Figure S3. H&E images of 2 mm thick control aorta #1, at 5x and 40x magnification. (a) Overall cross section (5x). (b) Tunica intima (40x). (c) Tunica media (40x). (d) Tunica externa (40x)

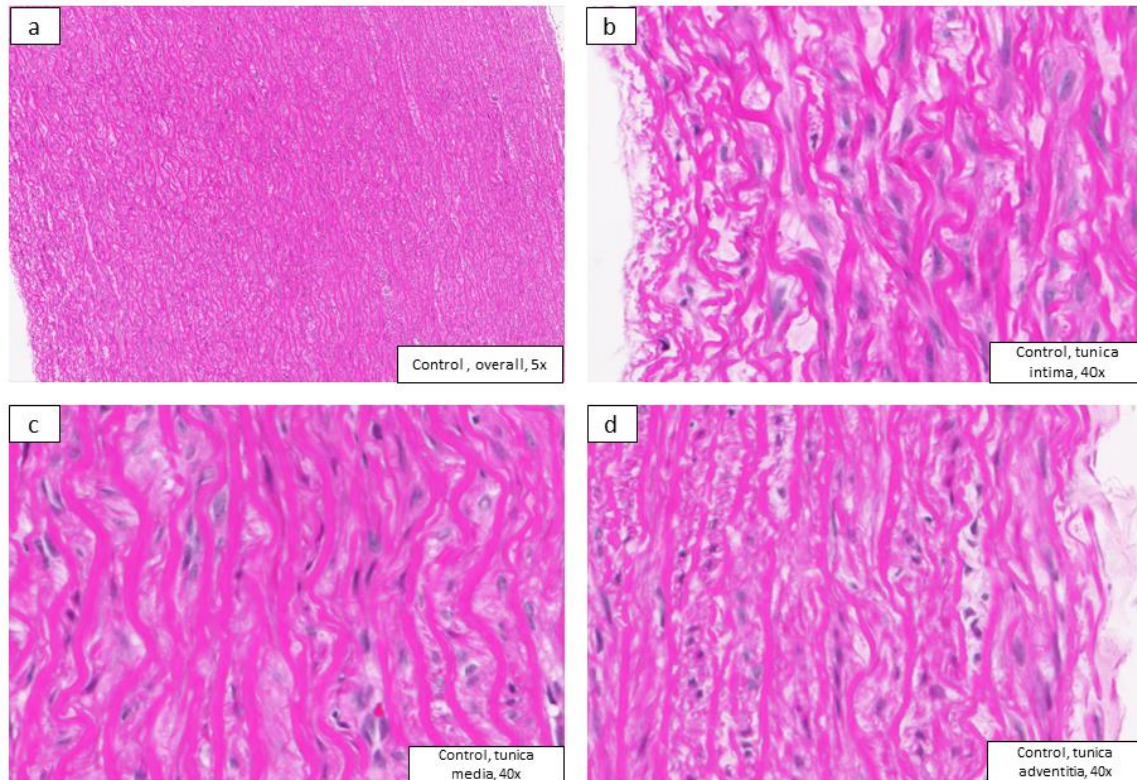


Figure S4. H&E images of 2 mm thick control aorta #2, at 5x and 40x magnification. (a) Overall cross section (5x). (b) Tunica intima (40x). (c) Tunica media (40x). (d) Tunica externa (40x).

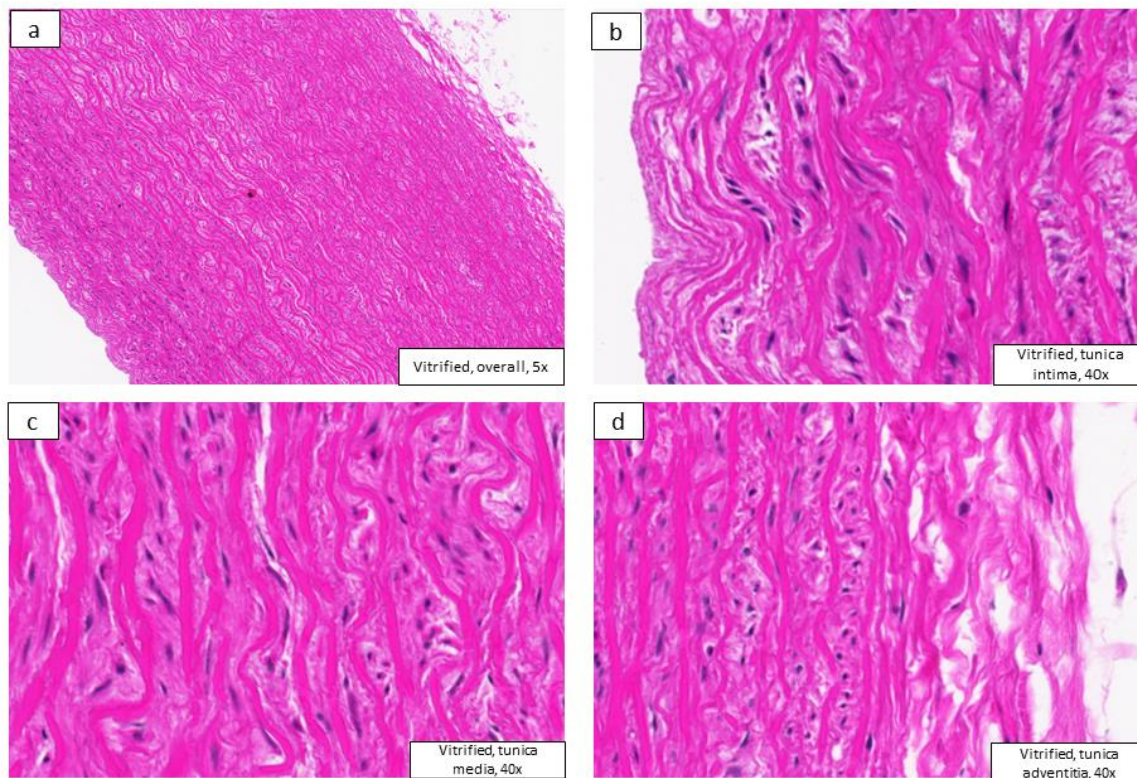


Figure S5. H&E images of 2 mm thick vitrified aorta #1, at 5x and 40x magnification. (a) Overall cross section (5x). (b) Tunica intima (40x). (c) Tunica media (40x). (d) Tunica externa

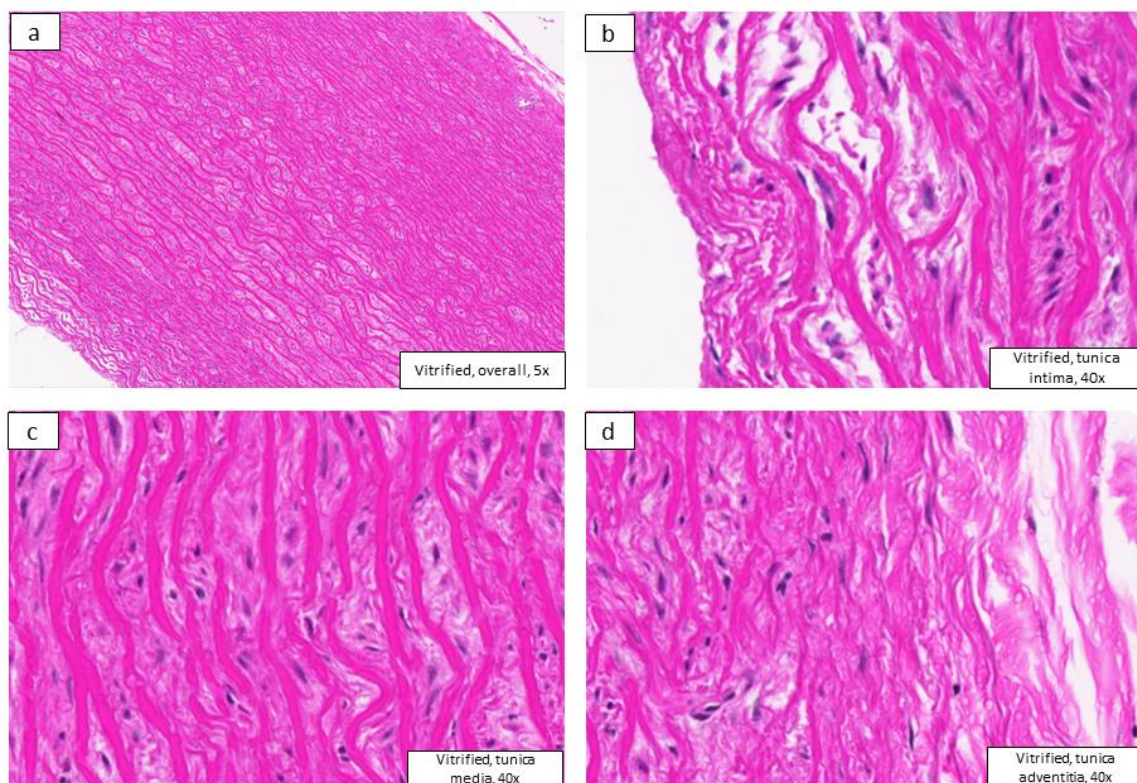


Figure S6. H&E images of 2 mm thick vitrified aorta #2, at 5x and 40x magnification. (a) Overall cross section (5x). (b) Tunica intima (40x). (c) Tunica media (40x). (d) Tunica externa

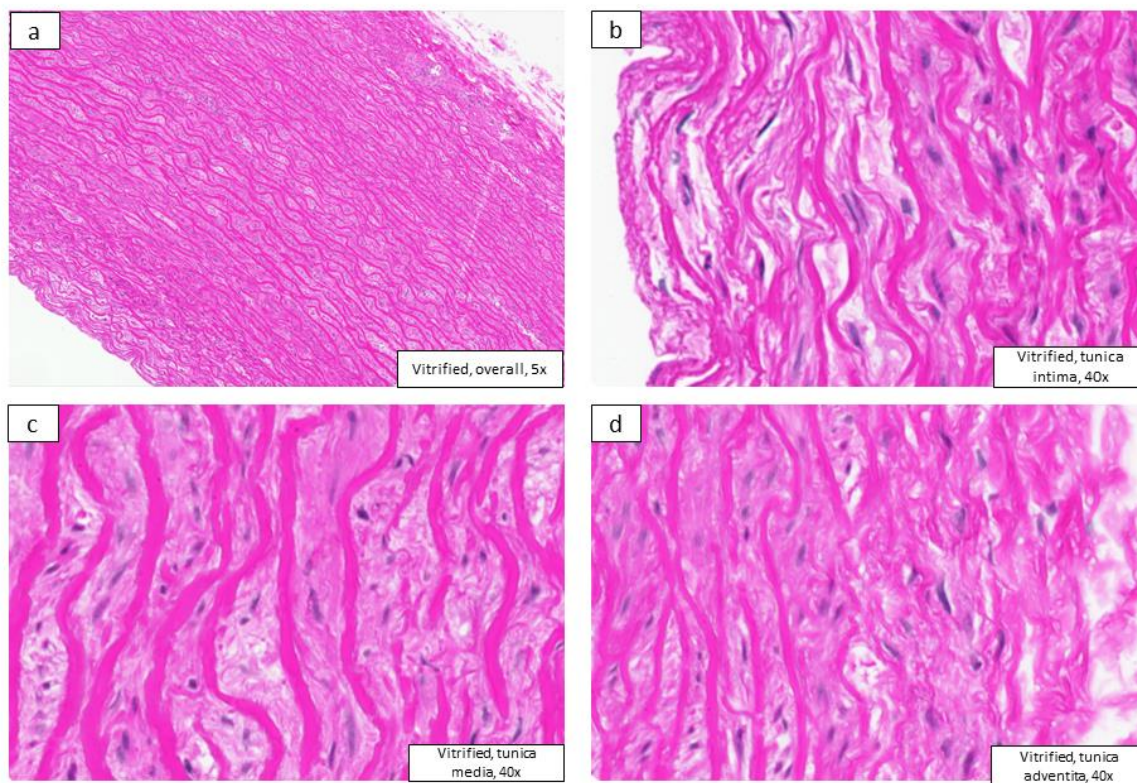


Figure S7. H&E images of 2 mm thick vitrified aorta #3, at 5x and 40x magnification. (a) Overall cross section (5x). (b) Tunica intima (40x). (c) Tunica media (40x). (d) Tunica externa

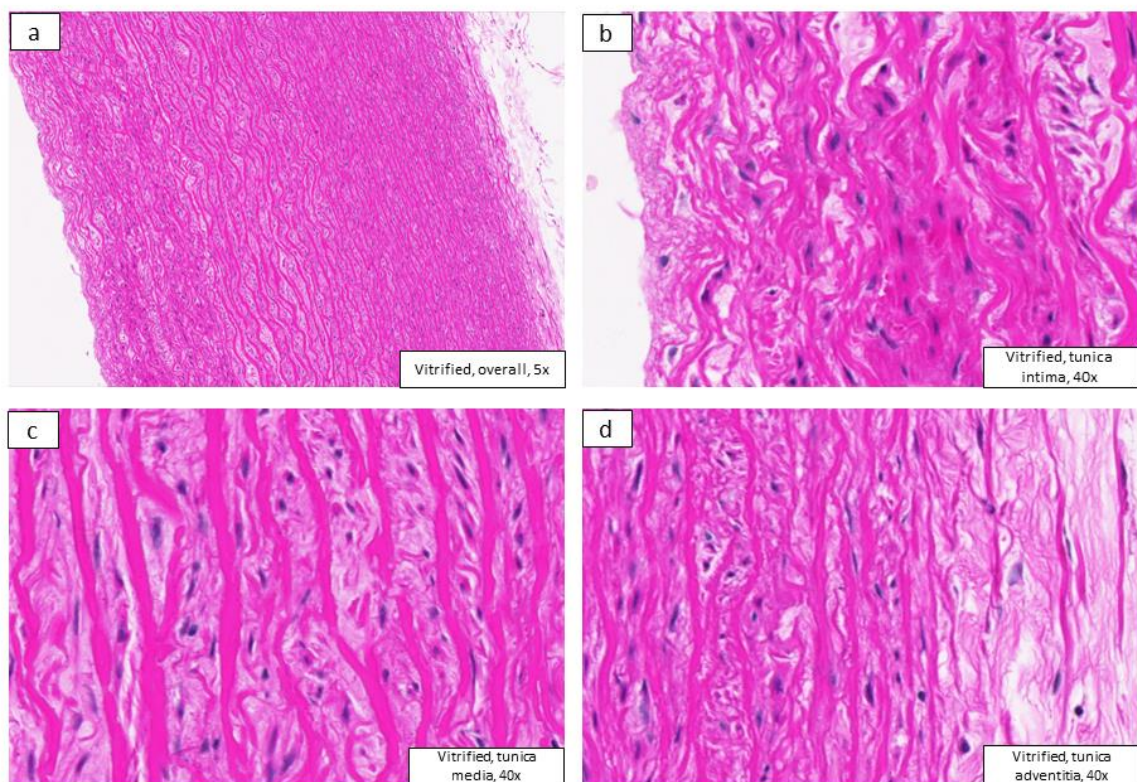


Figure S8. H&E images of 2 mm thick vitrified aorta #4, at 5x and 40x magnification. (a) Overall cross section (5x). (b) Tunica intima (40x). (c) Tunica media (40x). (d) Tunica externa

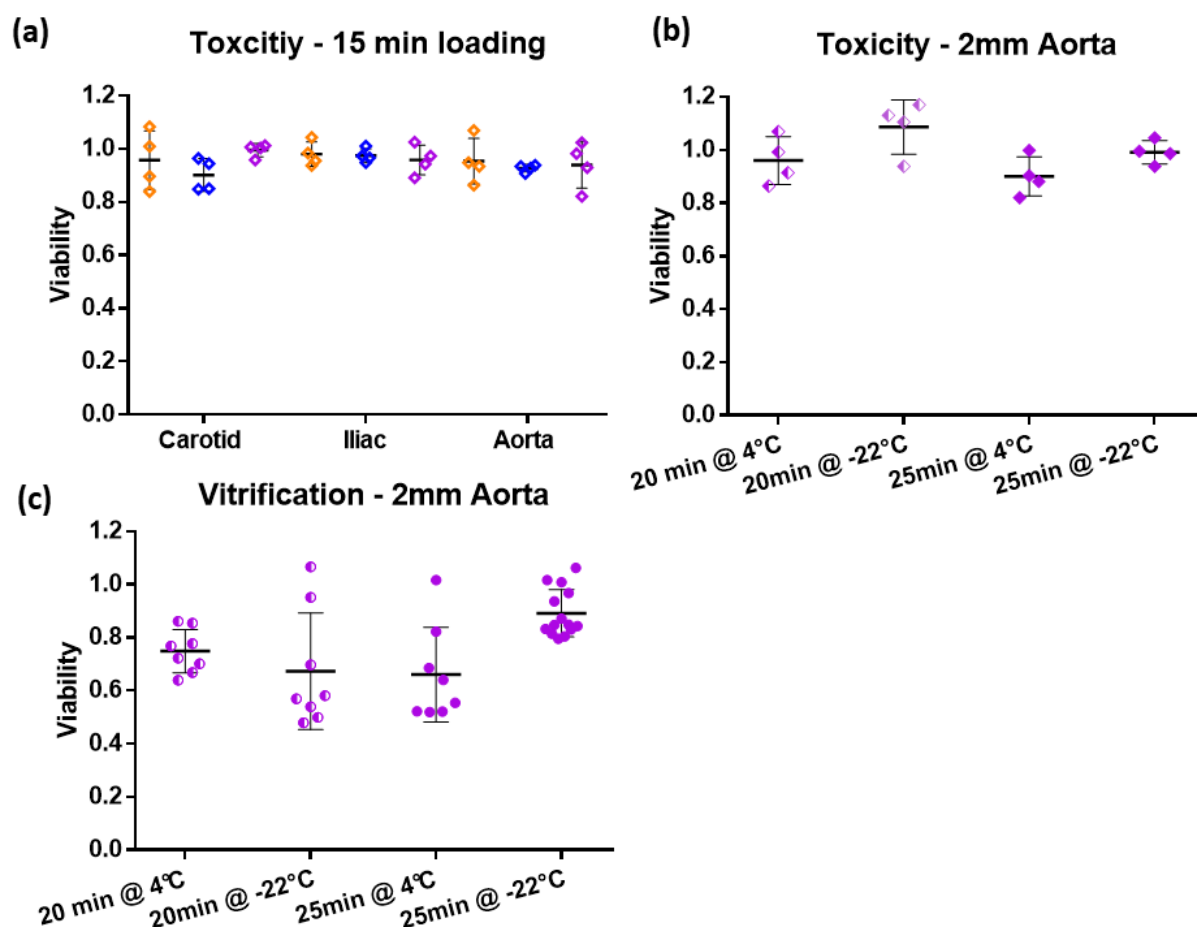


Figure S9. (a) 15 min step-wise loading of 3 types of CPAs (DP6, VS55, and M22) to 3 types of arteries (carotid, iliac, aorta) (n=4). (b) 2 mm aorta CPA toxicity study for different loading situations (n=4). (c) The viability corresponding to loading conditions in (b) after cryopreservation and rewarmed by AI heating at 30 kA/m (n=8 to 14). Data presented as mean \pm SD, p-values are calculated using one-way ANOVA with Tukey's multiple comparison tests. Temperature indicated in (b) and (c) represents the temperature of the last loading step, either 4 °C or -22 °C. Symbols are the same as in Figure 7.

Figure S9 demonstrates that step loading (each step 15 minutes) of any CPA causes negligible toxic damage to any of the arteries. The viability results of the toxicity study showed all three types of tissues with more than 90% viability measured by alamarBlue after the step loading with CPA. All 9 toxicity groups showed no significant difference compared to controls. For carotid arteries, $p = 0.9067$, 0.1716 and 0.9999 for DP6, VS55 and M22 treated groups, respectively. For iliac arteries, $p = 0.9978$, 0.9942 and 0.9210 for three CPA groups, respectively. For aorta, $p = 0.8739$, 0.4619 and 0.6543 for three CPA groups, respectively.

To cryopreserve the 2-mm thick aorta, we used M22 and elongated each loading step to 20 min or 25 min. The prolonged loading times could result in increased toxicity, so we placed the arteries with M22 in -22 °C when they reached the last loading step (full strength M22). However, while reduced temperature reduces the toxicity, it also slows diffusion activity, which leads to more difficulty in vitrification and rewarming. Therefore, whether or not to reduce the loading temperature is a balance between the toxic and diffusive effects.

In order to determine the best loading temperature for 20 and 25 min step loading, we did four groups of toxicity study: 20 min step-loading of M22 with the last step at 4 °C or -22 °C; and 25 min step-loading with the last step at 4 °C or -22 °C, as shown in Figure S9 (b). For both 20 and 25 min step loading, the groups loaded at 4 °C had a slight viability drop compared to the groups loaded at -22 °C. Then we added the vitrification and rewarming process to the four loading conditions with the viabilities shown in Figure S9c. For 20 min step loading, the diffusion activity inhibition had more influence on the cryopreservation while toxicity activity was acceptable, so adopting 4° C as the loading temperature was optimal. However, for 25 min step loading, the toxicity started to become significant, so we used -22 °C as the loading temperature at the last step.

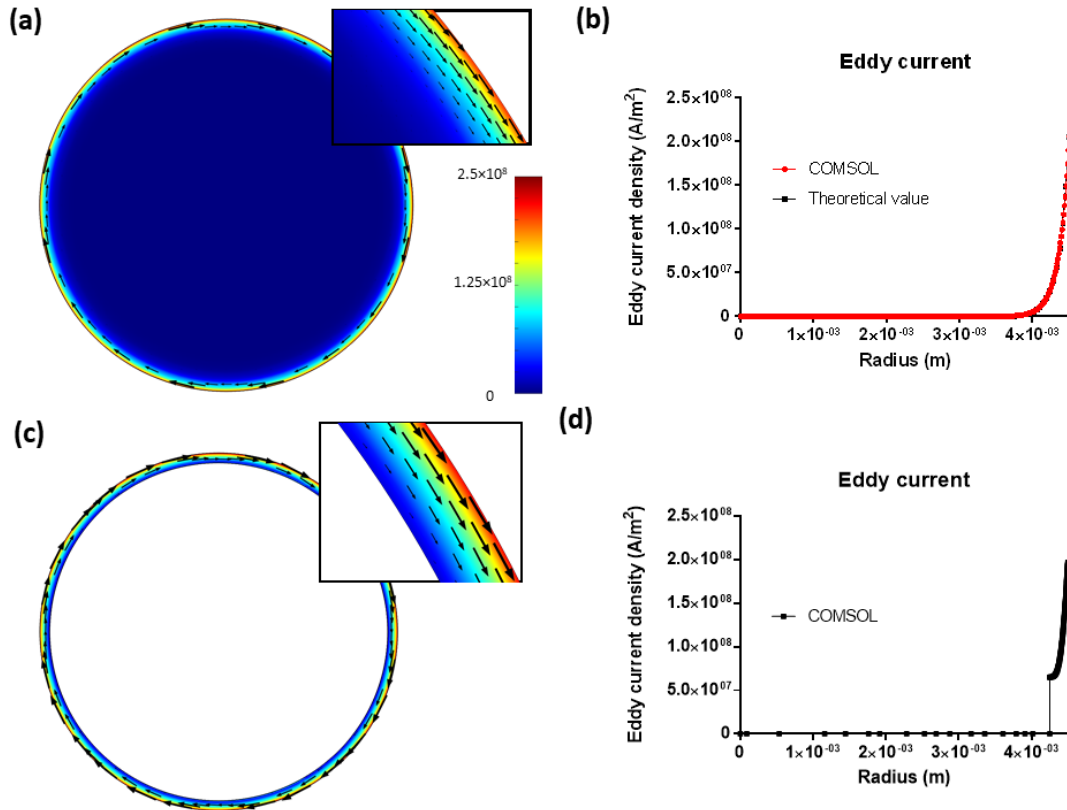


Figure S10. Induced eddy current distribution in solid and hollow cylinders under $H=20$ kA/m, 360 kHz. (a) Solid cylinder ($r = 4.5$ mm) eddy current modeled by COMSOL. (b) Comparison of radial current density between theoretical calculations and the COMSOL model. (c) Hollow cylinder ($r_{\text{out}} = 4.5$ mm, thickness = 0.25 mm) eddy current modeled by COMSOL. (d) Radial current density by COMSOL.

In this paper, we optimized the Al foil thickness and increased the magnetic field strength to obtain a higher warming rate than previous study. The Joule heating is linear to eddy current's square, therefore, in order to study the heating rate, we need to obtain the eddy current inside the Al foil.

The induced eddy current distribution inside a solid cylinder can be predicted by either theoretical calculation or COMSOL modeling. For theoretical calculation, we started from Maxwell's equations to obtain the governing equation for magnetic field:

$$\frac{\partial^2 H_z}{\partial r^2} + \frac{1}{r} \frac{\partial H_z}{\partial r} = \sigma \mu \frac{\partial H_z}{\partial t} \quad (\text{S1})$$

The boundary conditions (BCs) for solid and hollow cylinder are different. For a solid cylinder, the BCs are

$$\begin{cases} H_z(a,t) = H_0 \cos(\omega t) \\ H_z(0,t) \rightarrow \text{finite} \end{cases} \quad (\text{S2})$$

where a is the radius of the solid cylinder. We introduced the complex form \tilde{H}_z to solve for the expression for H_z and obtain the real part of the solution. The full derivation was described in Knoepfel's book. The solution is

$$\text{Re}(\tilde{H}_z) = H_z(r,t) = H_0 \cdot \left| \frac{J_0(\underline{R})}{J_0(\underline{R}_a)} \right| \cdot \cos(\omega t + \alpha) \quad (\text{S3})$$

where J_0 is the 0 order Bessel function. From Faraday's law in Maxwell equation, we get the current density j_ϕ

$$j_\phi = -\frac{\partial H_z}{\partial r} = -H_0 \cdot \frac{\partial}{\partial r} \left| \frac{J_0(\underline{R})}{J_0(\underline{R}_a)} \right| \cdot \cos(\omega t + \alpha) = \frac{\sqrt{2}}{\delta} H_0 \left| \frac{J_1(\underline{R})}{J_0(\underline{R}_a)} \right| \cos(\omega t + \alpha) \quad (\text{S4})$$

where δ is the skin depth, $\delta = \sqrt{1/\pi f \mu \sigma}$. For our study, if we applied the parameters for aluminum and the magnetic frequency of 360 kHz, we obtained a skin depth of 0.1365mm. We drew the eddy current density along the radius by Matlab and compared the curve with the results obtained from COMSOL and found a very good match, which verifies the validity of COMSOL model. From equation (S4), we can tell increasing the magnetic field will linearly increase the current density, therefore, in order to achieve a higher heating, we increased the magnetic field from 20 kA/m to 30 kA/m. In addition, we changed the Al foil thickness from previous 0.1 mm to present 0.25 mm, which is larger than the skin depth in order to take full advantage of the heating performance.

For a hollow cylinder, the theoretical solution is very difficult to obtain. Therefore, we only used COMSOL to obtain the current density, and it behaves similar to the solid cylinder. For further study, we will try to obtain the theoretical solution or the approximate form for the eddy current density in the hollow cylinder, then combine it with heat transfer equation to optimize aluminum foil thickness in order to best utilize the space and generate enough heat.

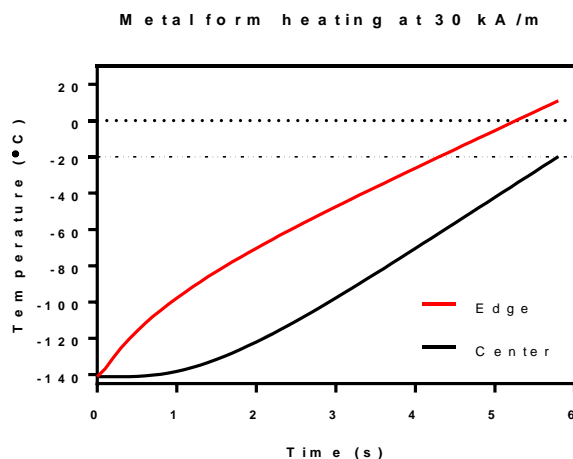


Figure S11. Thermal history of the center and the edge of the 2 mm thick aorta heated by metal form heating at 30 kA/m.

Figure S11 shows the thermal history of the center and edge of the aorta heated by metal form heating at 30 kA/m, which is the situation where the largest temperature differential occurs. The largest temperature differential is 52.1 °C at 2.3s after we start the rewarming (edge is -63.2 °C, and center is -115.3 °C). The estimates the maximal thermal stress due to this temperature change as 2.03 MPa, which is less than the critical tensile stress (3.2 MPa), making cracking unlikely.

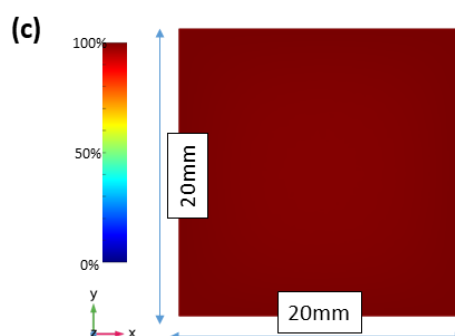
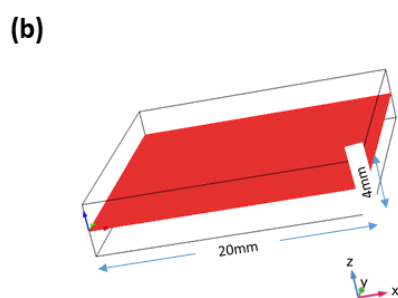
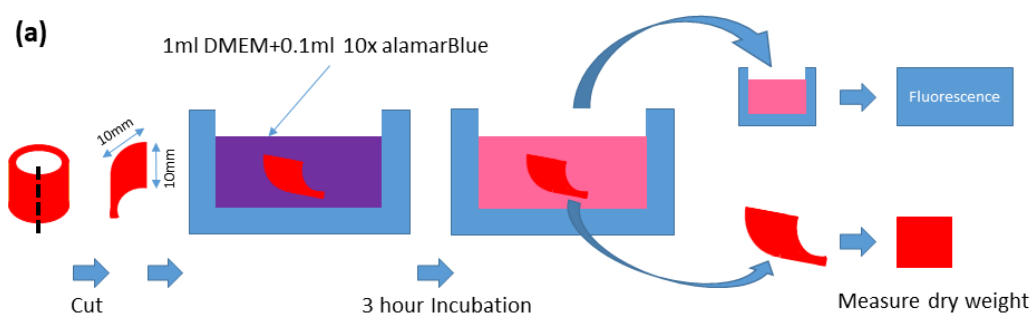


Figure S12. (a) AlamarBlue viability test protocol. (b) AlamarBlue diffusion model, doubled thickness of 2-mm aorta to simulate the diffusion in and diffusion out processes. The red plane represents the center plane of the model. (c) AlamarBlue concentration at the center plane after 3-hour incubation, representing the capability of the AlamarBlue to diffuse in and out of 2-mm aorta.

Figure S12a shows the process of incubating an artery and measuring the fluorescence. Figure S12b shows the diffusion model of alamarBlue to arteries during 3 hours of incubation at 37 °C. Considering the increased temperature, the diffusion coefficient was assumed to be 10 times higher than that of CPA at 4 °C, with a value of $6.5 \times 10^{-10} \text{ m}^2/\text{s}$. In order to measure the viability at the center of a 2-mm thick aorta, the alamarBlue needs to diffuse in and out within 3 hours. To simplify the modeling, we doubled the thickness of the aorta (shown in Figure S12b) from 2 mm to 4 mm so that the alamarBlue concentration in the center region of this model will simulate diffusion in and diffusion out. We also doubled the length of the aorta to decrease the edge effect. The center region is fully diffused by alamarBlue after 3 hours, shown in Figure S12c, which means the alamarBlue is able to diffuse in and out of the 2 mm thick aorta, demonstrating that this viability assay can represent the whole tissue on average.